

## The use of hydrogen to supply combustion engines – part 1

### ARTICLE INFO

Received: 22 April 2025  
Revised: 26 September 2025  
Accepted: 21 November 2025  
Available online: 14 January 2026

Key words: *hydrogen, combustion engines, fuel cell, exhaust gas emissions*

This is an open access article under the CC BY license (<http://creativecommons.org/licenses/by/4.0/>)

### 1. Introduction

Stringent emission standards, with pollution levels closely linked to the combustion quality of existing internal combustion engines (ICEs), force manufacturers to develop new fuel injection solutions and adapt existing ones to meet more stringent standards [13]. Furthermore, other solutions are being sought to meet stringent emission standards. Nowadays, hydrogen ( $H_2$ ) is increasingly being used to power ICEs in various types of vehicles and stationary applications. The development of the energy and transportation sectors has increased interest in using fuels derived from renewable sources, rather than fossil fuels.

Menes [68] conducted a synthetic review of the political framework, specifically the operational plans and initiatives, along with national leadership for the advancement of  $H_2$  technologies and efficiency in 19 countries.

Gis and Gis [36] explored the circumstances surrounding—the adoption of hydrogen in transportation in North-western Europe. Taking into account various technical aspects—including hydrogen refueling stations (HRS) and fuel cell electric vehicles (FCEVs), and economic factors (such as  $H_2$  usage costs), the following countries were included: Belgium, Denmark, France, Germany, the Netherlands, Norway, and England. In Poland, significant fuel and energy corporations (including Orlen, Lotos, PGNiG, and ZE PAK Capital Group) are highly interested in the application of  $H_2$  in transportation, while vehicle manufacturers such as Solaris and Autosan are focused on developing vehicles with fuel cells (FCs). It was discovered that the optimal placement of basic  $H_2$  refueling stations is situated along the TEN-T corridors traversing Poland. The sequence of such locations is as follows: 1 – Poznan, 2 – Warsaw, 3 – Białystok, 4 – Szczecin, 5 – Łódź region, 6 – Tricity, 7 – Wrocław, 8 – Katowice region, 9 – Kraków.

Sikora and Orliński [98] observed that on 28 March 2023, the EU Council approved a rule imposing strict  $CO_2$

*Hydrogen is used to supply various internal combustion engines, as well as to fuel cells, which are employed in various vehicles. The goal of the present study was to review the state of art relative to the application of  $H_2$  in the automotive industry. The review focuses on out-of-engine studies on the effect of  $H_2$  combustion processes, internal combustion engines supplied with  $H_2$ , and vehicles utilizing fuel cells. Challenges in applying fuel cells to actual vehicles include limited flexibility in controlling power flow in the PEMFC + B setup, significant power flow losses, which complicate the management of energy systems in case of. The PEMFC + B + UC configuration, as well as a low power density of batteries. A drawback of  $H_2$  engines is the emission of  $NO_x$ , which can be lowered by exhaust gas treatment. Fuel cell vehicles (FCVs) can be a clean energy alternative to gasoline-powered cars. However, their development depends on  $H_2$  fuel availability and the expansion of refueling infrastructure.*

emission norms for new cars and vans; therefore, from 2035 onward, only electric or  $H_2$ -fueled cars and vans will be eligible for registration. Notably, hydrotreated vegetable oil was excluded as a fuel from the Fit for 55 package regarding cars and vans. This type of fuel can replace diesel with HVO fuel without affecting the fuel injection (FI) control system and also has significant potential to reduce greenhouse gas emissions.

Various techniques used for the extraction of  $H_2$  from biomass are reviewed in [74].

Skobiej [99] reviewed the most recent studies and progress in utilizing  $H_2$  as fuel for internal combustion engines. The review thoroughly examined  $H_2$ 's ability to enhance combustion efficiency, particularly when mixed with  $NH_3$  or  $CH_4$ . Essential findings emphasize  $H_2$ 's potential to reduce detrimental emissions, such as  $CO$ ,  $HC$ , and soot, while it may increase  $NO_x$  emissions due to elevated combustion temperatures. The article also examines different  $H_2$  injection methods, such as direct injection (DI), which surpasses port fuel injection (PFI) by notably improving power production and fuel efficiency. Additionally, the research highlights the importance of adjusting  $H_2$  ratios in dual-fuel ICEs to achieve a balance between efficiency and emissions. These findings underscore the importance of  $H_2$  in future decarbonization initiatives, with ongoing studies focused on reducing  $NO_x$  emissions while maintaining high efficiency.

Wesołowski et al. [130] suggested producing  $H_2$  through the gasification of electronic waste in a steam environment to create syngas, which can serve as a  $H_2$  source after isolation processes. They showcased the outcomes of gasifying electronic waste, which includes plastic components or epoxy resins, detailing the composition of the syngas produced during recycling and evaluating the possibilities of this waste processing for fueling transportation.

Matla et al. [66] examined the current understanding of H<sub>2</sub> combustion systems, which are now quite popular, primarily because of the advanced production technology and comparatively low recycling costs of FCs. The authors examined existing solutions that address challenges associated with H<sub>2</sub> production, storage, and transport. They stated that the forecasted threefold increase in H<sub>2</sub> production by 2050, driven by decreasing production costs, promotes research focused on its application as a fuel for H<sub>2</sub> ICEs.

Stępien [103] reported that H<sub>2</sub>, being a zero-emission fuel, enables the construction of a piston ICE that meets the criteria for "Zero Emission Vehicles" regarding CO<sub>2</sub> emissions. The piston ICE powered by H<sub>2</sub> could serve as a bridging technology for powertrains, particularly in trucks and off-road vehicles, competing with both electric drives and FCs. The author offered a comprehensive examination of the potential advancement and distribution of H<sub>2</sub>-fueled ICEs in automobiles.

A separate development group consists of vehicles utilizing hydrogen via FCs, known as fuel-cell electric vehicles (FCEVs) [28], some of which are in the early stages of development. Daszkiewicz and Kołodziejek [24] examined the option of utilizing ultracapacitors, batteries, or FCs to enhance the efficiency of a rail vehicle's powertrain. The choice of the right solution relies on the vehicle's intended purpose and its traction features. Zadraż et al. [134] simulated dynamic loads on the propulsion system of ships equipped with unconventional power systems – reformed methanol FCs (RMFCs).

The present study reviews the state of art regarding the application of H<sub>2</sub> in the automotive industry. The review focuses on out-of-engine studies on the effect of H<sub>2</sub> combustion processes, internal combustion engines supplied with H<sub>2</sub>, and vehicles powered by FCs.

## 2. Out-of-engine studies on the effect of H<sub>2</sub> combustion process

### 2.1. General overview and key mechanisms

Out-of-engine studies on H<sub>2</sub> combustion processes are conducted numerically or on test stands, including dedicated burning chambers.

Habib et al. [38] compared various H<sub>2</sub> combustion mechanisms elaborated by various researches, including GR13.0 [116], Dagaut et al. [22], ÓConaire et al. [75], Zsély et al. [138], Davis et al. [25], Saxena & Williams [94], Sun et al. [105], Li et al. [58], Ahmed et al. [2], USC-II [126], Konnov [52], Rasmussen et al. [86], Starik et al. [102], NUIG-NGM [42], Hong et al. [45], SanDiego [21], Burke et al. [18], CRECK [114], Kéromnès et al. [49].

ÓConaire et al. [75] developed a comprehensive kinetic model for H<sub>2</sub>/O<sub>2</sub> combustion across a wide range of temperatures (298–2700 K), pressures (0.05–87 atm), and equivalence ratios (0.2–6). This extensive system and evaluation examined combustion characteristics across a range of temperatures, from low to high, and pressures, from sub-atmospheric to elevated, for fuel-lean to fuel-rich mixtures. Their rigorous assessment provided insights into essential reaction pathways across various combustion conditions, relevant to both basic kinetics and real-world applications.

Li et al. [59] conducted an in-depth analysis of the chemical reaction dynamics for H<sub>2</sub>/O<sub>2</sub> combustion, referencing previous research [15] and utilizing new kinetic and thermodynamic data. Their mechanism was tested under various experimental conditions, including shock tubes, flow reactors, and laminar premixed flames. They determined that the H + OH + M reaction is crucial, particularly for simulating high-pressure flame propagation, as flame speeds were matched by employing different transport coefficients from the literature, with adjustments made to the rate within acceptable uncertainty.

The mechanism of the H<sub>2</sub>/O<sub>2</sub> reaction is essential for both basic kinetics studies and practical combustion applications such as fire safety, energy conversion, and stimulus [59]. The application of H<sub>2</sub> as a fuel in these sectors requires knowledge of its oxidation chemistry. Moreover, the fundamental reactions involving the species H, O, OH, HO<sub>2</sub>, and H<sub>2</sub>O<sub>2</sub> are crucial for forming the reactive radical pool that initiates oxidation in HC fuels. Thus, enhancing H<sub>2</sub>/O<sub>2</sub> kinetics provides a better understanding of the combustion process and advances H<sub>2</sub>-oriented technologies in various sectors [75]. The H<sub>2</sub>/O<sub>2</sub> reaction mechanism is explained in [59].

### 2.2. Recent advances in H<sub>2</sub> combustion chemistry

Recently, several studies have enhanced the comprehension of H<sub>2</sub> combustion chemistry [53]. In the reaction H<sub>2</sub> + OH = H<sub>2</sub>O + H, studies [67, 106, 129], showed strong consistency with prior experimental findings. Nonetheless, the discrepancies in the determined rate constants were greater than those used in kinetic models from 2015 [53], making it difficult to choose a revised expression. An experimental investigation conducted between 295 and 701 K on the reaction OH + OH = H<sub>2</sub>O + O, which is not part of a [53, 118, 119] H<sub>2</sub> kinetic mechanism, found that the rate constant from the study by Sangwan and Krasnoperov [93] below 834 K was less than other recorded measurements. The low-temperature rate constant was in agreement with the theoretical study conducted by Nguyen and Stanton [72]. Another study [5] suggested a fit to such data, indicating strong alignment with high-temperature tests by Wooldridge et al. [131] and a reverse rate from Sutherland et al. [107]. Hong et al. [44] also supported the findings of Wooldridge et al. [131].

Konnov [52] analyzed recent proposals by Burke and Klippenstein [19, 51] regarding the influence of chemically termolecular reactions, such as H + O<sub>2</sub> + R, on H<sub>2</sub> combustion kinetics under typical conditions. These reactions require careful consideration for inclusion in mechanisms, as they alter reactivity and laminar flame speeds. To investigate this, a comprehensive H<sub>2</sub> combustion mechanism was assessed to mitigate increased chain termination from these reactions while preserving or enhancing model performance. Revised kinetic investigations led to the inclusion of four new reactions and modifications to three rate constants, although this significantly decreased the computed burning velocities compared to experiments and earlier models, primarily due to termolecular reactions. The introduction of a theoretical transport database from Jasper et al. [47, 48] greatly improved the accuracy of the revised model, aligning it closely with experimental burning speed data

for H<sub>2</sub>+air flames at atmospheric pressure, representing a notable advancement over previous models [54]. The system included new termolecular reactions and revised rate constants for existing reactions. These chemical changes did not significantly affect the mechanism's ability to simulate H<sub>2</sub> self-ignition and oxidation behavior in flow reactor setups.

Olm et al. [76] systematically evaluated 19 H<sub>2</sub> combustion mechanisms using an extensive experimental dataset, including ignition delays, species profiles, and burning speeds. They established error function values to assess the effectiveness of each mechanism across different test datasets, with values closer to one indicating better performance.

According to the average error function values, the Kéromnès [49] mechanism provides the most accurate predictions for ignition delay times and burning speeds, while the flow reactor data was best represented by the Starik [102] mechanism. Overall, the Kéromnès-2013 mechanism demonstrated the highest efficiency, closely followed by NUIG-NGM [42], Konnov [52], and Li et al. [58].

### 2.3. CFD modeling and engine performance findings

Simulations in computational fluid dynamics (CFD) indicate that DI ICEs achieve a 40% increase in brake power, resulting from a 30.6% improvement in volumetric efficiency. Additionally, DI systems reduce NO<sub>x</sub> emissions by 36% compared to port fuel injection (PFI) with H<sub>2</sub> at an optimal air/fuel (A/F) ratio ( $\lambda$ ) of 1.5. The research also highlights H<sub>2</sub>'s superior efficiency in reducing fuel consumption – by 71.8% compared to CH<sub>4</sub> and 67.2% compared to coke oven gas (COG) – due to its higher heating value per unit mass [71]. The significant 71.8% decrease in brake-specific fuel consumption observed with H<sub>2</sub> DI compared to CH<sub>4</sub> is mainly attributed to H<sub>2</sub>'s higher energy density. The precision of the DI system further amplifies this effect by optimizing the combustion process, minimizing fuel waste, and increasing thermal efficiency. These results were obtained for an optimal A/F ratio ( $\lambda = 1.5$ ), maximizing the benefits of H<sub>2</sub>'s exceptional combustion properties.

### 2.4. Influence of H<sub>2</sub> enrichment and combustion strategies

Gharehghani et al. [35] numerically studied the effect of H<sub>2</sub> enrichment on the operational range and combustion characteristics of a spark-ignition (SI) ICE powered by natural gas (NG). They found that misfiring occurred at equivalence ratios of approximately 0.61, 0.48, and 0.42 for H<sub>2</sub> fractions of 0%, 30%, and 50%, respectively. Combustion durations were 70, 47, and 45° crank angle for H<sub>2</sub> contents of 0%, 30%, and 50%, respectively, at the same equivalence ratio ( $\Phi = 0.625$ ). The highest brake-specific NO<sub>x</sub> was observed at  $\Phi = 0.83$  ( $\lambda = 1.2$ ), and this value was nearly unaffected by the H<sub>2</sub> fraction. Increasing the H<sub>2</sub> fraction reduced emissions of CO, HC, and CO<sub>2</sub>. Adding 30% H<sub>2</sub> reduced CO<sub>2</sub> emissions by 10.2%, while a 50% H<sub>2</sub> fraction led to a 22.7% reduction.

Matla et al. [66] proposed a conceptual H<sub>2</sub> combustion system for ICEs, utilizing a prechamber to improve combustion parameters and overall engine efficiency. As noted

in [65], a split combustion chamber solution enhances the controllability of the combustion process in H<sub>2</sub> ICEs. Such a system is theoretically more efficient than any previously known solution. It was determined that the compression ratio (CR) and the degree of mixture depletion have the most significant impact on the H<sub>2</sub> combustion process. Their influence on H<sub>2</sub> knock formation was assessed, which can be categorized as severe knock (highly undesirable) or mild knock, depending on the level of pressure oscillations in the combustion chamber; in the latter case, combustion improvement is possible.

Brzeżański et al. [14] studied the combustion of H<sub>2</sub>-air mixtures with varying compositions. After H<sub>2</sub> DI was introduced into an isochoric combustion chamber, the mixture formed during the combustion process. The effect of fuel dose distribution before and after ignition on fire front development and pressure behavior in the isochoric chamber was analyzed. Management of the H<sub>2</sub>-air mixture's combustion, primarily related to flame front velocity and heat release rate, can be achieved by using DI and initiating combustion during fuel injection. This method enables the delivery of stoichiometric mixtures to ICEs, significantly increasing the heat produced by the engine without entering the abnormal combustion zone. This can enable high engine performance compared to engines running on lean mixtures. Filming and pressure recording in the isochoric chamber were used to study combustion, demonstrating the effectiveness of this approach for analyzing mixture formation and combustion.

### 2.5. Advanced injection strategies and emissions control

Using CFD modelling, Shi et al. [96] analyzed how different injection parameters – including the amount of H<sub>2</sub> per pulse, the inter-pulse interval, and the width of the minor injection pulse – affect engine efficiency and emissions. The results indicate that split DI enhances mixture stratification, resulting in faster and more efficient combustion than single injection. Increasing the mass fraction of post-injection and the interval between injections further improves combustion, as a longer minor injection pulse width enhances engine efficiency by enriching the mixture near the spark plug. However, while this approach reduces HC and CO emissions to nearly negligible levels, it increases NO<sub>x</sub> emissions.

Shahpouri et al. [95] reported that to minimize NO<sub>x</sub> and soot emissions from engines running on hydrogen, an engine can be enhanced with a hardware-in-the-loop (HIL) configuration, thereby reducing calibration work for the engine. Furthermore, optimal model-based combustion control (MCC) can lower engine-out emissions. Both HIL and MCC methods need rapid and precise models for NO<sub>x</sub> and soot emissions. The precision of a rapid physics-based engine model utilizing premixed combustion relies on forecasting the laminar flame speed (LFS). The authors forecasted LFS using an artificial neural network (ANN) machine learning (ML) approach. The LFS model and the engine combustion model are validated for both an H<sub>2</sub> SI engine and an H<sub>2</sub>-diesel CI engine. The black-box and gray-box models for soot and NO<sub>x</sub> emissions were created for the H<sub>2</sub>-diesel engine utilizing ANN, support vector machine (SVM), and Gaussian process regression (GPR) techniques

with various feature sets, and are then compared to a standard one-dimensional physics-based  $\text{NO}_x$  model. The gray-box emission models were ideal for engine HIL configurations where precision is crucial. The black-box models were appropriate for model-based real-time control of  $\text{H}_2$  combustion when computational power is restricted.

## 2.6. Syngas combustion and engine adaptation

Hagos et al. [39] analyzed the properties of three distinct syngases derived from major gasification products of low and medium calorific values, comparing them to CNG and  $\text{H}_2$ . Syngases, especially those with a medium calorific value, have an adiabatic flame temperature similar to that of  $\text{H}_2$ , resulting in increased  $\text{NO}_x$  emissions. Syngases have a much lower stoichiometric A/F ratio compared to CNG and  $\text{H}_2$ , which may increase brake specific fuel consumption (BSFC).

Fiore et al. [29] reported that syngas fuel serves as an intermediary phase in the transition from carbon-based to  $\text{H}_2$ -derived fuels. Syngas-powered dual-fuel engines achieve notable standard fuel savings. Syngas has low knocking propensity and allows the use of high compression ratios (CRs). Its broad flammability range favors lean combustion. Dual-fuel CI engines, homogeneous charge spark ignition engines, and DI SI engines are highly sensitive to the physical and chemical properties of syngas, such as CO and  $\text{H}_2$  content, laminar flame speed, broad flammability range, and lower density compared to air. The authors also noted that large-eddy simulations or even direct numerical simulations should be conducted, and models require further improvement and validation. Models addressing turbulence-chemistry interaction should be tested, especially for high-speed DI of syngas. Multicomponent diffusion models should be included, as  $\text{H}_2$  diffuses much faster than other mixture components. Intake and exhaust processes, typically neglected in syngas port-injection engine simulations, must be considered, as a significant part of power derating is linked to reduced volumetric efficiency. These processes must be included in high-fidelity data assessment.

Paykani et al. [78] examined the impact of syngas use on the performance and emissions of SI, CI, HCCI, and advanced dual-fuel engines like reactivity-controlled compression ignition (RCCI) engines. Many factors affecting both syngas and engine properties significantly influence the prospective benefits of syngas use in ICEs. Variations in the  $\text{H}_2$  fraction of syngas have limited its broad application. Additional gaseous components, such as  $\text{CO}_2$ ,  $\text{N}_2$ , and  $\text{CH}_4$ , in syngas may negatively impact engine combustion. The key reasons for power loss in SI engine are the low energy density of syngas/air blends and reduced volumetric efficiency due to air replacement. Adding high  $\text{H}_2$ -content syngas as a secondary fuel improved combustion and performance compared to low  $\text{H}_2$ -content syngas. Using high CRs in syngas-powered engines reduced power loss without increasing knocking. DI of syngas can also eliminate power derating, avoiding issues related to reduced volumetric efficiency and unintentional pre-ignition or surface ignition in the intake system.

## 2.7. Material issues: hydrogen embrittlement

As noted by [89], the intended replacement of conventional fuel in combustion engines with  $\text{H}_2$  may cause hydrogen embrittlement, particularly in various steel-based materials, depending on material type, structure, and operating conditions. The authors described the process of electrochemical hydrogenation, similar to galvanic coating of metals used in the automotive industry. They assessed how hydrogenation duration affects the properties and microstructure of austenitic steel. They found that the material was strengthened by electrochemical hydrogenation in a 0.5M  $\text{H}_2\text{SO}_4$  solution. The increase in strength was directly related to the amount of  $\text{H}_2$  supplied. However, the typical features of hydrogen embrittlement, such as localized brittle fracture areas reported in the literature, were not observed in the analyzed material.

## 2.8. Summary and research directions

Several mechanisms describing  $\text{H}_2$  combustion have been published recently, exhibiting varying degrees of complexity and accuracy.

Various out-of-engine studies on the effect of  $\text{H}_2$  combustion have utilized CFD methods, investigating not only pure  $\text{H}_2$  but also gases containing high  $\text{H}_2$  content, such as syngases.

The application of combustion engines fuelled with  $\text{H}_2$  and fuel cells (FCs) in vehicles is discussed in the following subchapters.

The use of the dual-fuel ICEs supplied with fuel and  $\text{H}_2$  is presented in Part 2 of this review. It can be noticed that the efficiency of such ICEs can be enhanced, for example, by applying new solutions to their injection system, such as a hypocycloid mechanism in the drive of pumping sections of high-pressure pumps for diesel combustion engines and the others [9, 12, 64].

## 3. Combustion engines supplied with $\text{H}_2$

Escalante and Fernandez [27] stated that in ICEs fueled by  $\text{H}_2$ , the emissions from air/ $\text{H}_2$  mixtures primarily consist of  $\text{CO}_2$  and  $\text{NO}_x$ . For  $\text{NO}_x$ , higher emissions occur because  $\text{H}_2$  combustion produces higher flame temperatures and flame speeds than other fuels, such as gasoline. Emissions of unburned hydrocarbons (UHC) result from the heating of lubricant oil and the use of oil-based coolants. The thermal efficiency of a  $\text{H}_2$ -fueled engine (38.9%) exceeds that of a gasoline engine (25%). The power output by a  $\text{H}_2$ -fueled test engine reached 80% of the output of a gasoline engine. At light loads,  $\text{H}_2$  combustion can minimize  $\text{NO}_x$  emissions and prevent abnormal combustion phenomena by shortening the injection duration and delaying the spark timing. Spark-ignition (SI) engines can operate efficiently with air- $\text{H}_2$  mixtures at equivalence ratios between 0.3 and 0.9, using compression ratios (CR) above 12:1, exhaust gas recirculation (EGR), shorter injection durations, and delayed spark timing. Nearly ideal functioning of compression-ignition (CI) engines requires increasing CR, using EGR, and primarily employing a combustion inducer (such as diesel) while adding an  $\text{H}_2$  mixture to achieve the desired power output. Replacing hydrocarbons requires research on CI engines powered by  $\text{H}_2$  and diesel, operating at CR above 15:1, using natural gas (NG) injectors, and variable

$H_2$  loads, starting from low loads until minimal HC levels are achieved, utilizing a combustion initiator.

From an engine design perspective, the primary modifications suggested for using  $H_2$  as a fuel include:

- Replacement of injectors: Larger injection volume capacity is needed. The low density of  $H_2$  necessitates rapid injection of larger fuel quantities. NG injectors can be modified to operate with  $H_2$ .
- Improved temperature management: The high combustion speed of  $H_2$ , compared to gasoline and diesel requires enhanced temperature control, such as cooling around nozzles, spark plugs, and cylinder heads.
- Mixtures: Using  $H_2$  combustion alongside hydrocarbons is recommended as an initial phase of  $H_2$  integration. Light blends with about 5–10%  $H_2$  by volume can serve as a starting point for a gradual, clean transition from traditional fuels.

Verhelst et al. [120] stated that due to its physical and chemical characteristics,  $H_2$  is primarily employed in SI applications and is regarded as a baseline. The power output of an  $H_2$  ICE is lower than that of a gasoline engine due to  $H_2$ 's low volumetric energy density.  $H_2$  occupies more engine volume, reducing the possible air intake per cylinder. This negative effect is partly offset by the higher heating value and stoichiometric air-to-fuel ratio, but it may still lead to a 17% reduction in power output. Although port fuel injection (PFI) has lower theoretical performance than other mixing systems, it remains the only system used in demo cars due to its simplicity and injector availability.

The authors further explained that the wide flammability range of  $H_2$  benefits load control strategy, enabling a 'qualitative' load control approach that eliminates the need for throttling and associated losses. In this case, the A/F ratio is raised to decrease performance at partial loads, which works similarly to a diesel engine. Running the ICE with very lean mixtures additionally helps reduce  $NO_x$  emissions. Reintroducing exhaust gases (EGR) to the inlet is another method to lower the performance at part-load operations without throttling. The presence of the inert exhaust gases also reduces the amount of air and fuel in the engine.  $H_2$  enables stable ICE operation with higher EGR levels than gasoline due to its broader flammability range and faster flame speed. The maximum power per engine displacement can be increased by raising inlet pressure using supercharging or turbocharging, with turbocharging being preferred for efficiency. However, the reduced throttle response and lower exhaust energy with  $H_2$  compared to traditional fuels create challenges for turbocharged  $H_2$  ICEs. Control methods based on power density or ICE efficiency are typically integrated into lean-burn and stoichiometric strategies. At low loads, the ICE operates with varying air-to-fuel (A/F) ratios, yielding high efficiency and very low emissions. When a specific power requirement is exceeded, the operation shifts to throttled stoichiometric mode. The performance achieved by this load control approach was reflected in a single-cylinder ICE map at BMW, later scaled to 12 cylinders in a demo car [122]. The map showed optimal performance between 4 and 6 bar IMEP (indicated mean effective pressure) with an indicated thermal efficiency (ITE) of 42%. This maximum efficiency is

paired with a large portion of the map showing ITE values above 38%. However, the maximum torque reached about 10.3 bar IMEP, indicating lower power density compared to similar gasoline ICEs, mainly due to low inlet charge density and combustion limitations.

The authors also noted that the broad flammability range, high flame speed, and low ignition energy of  $H_2$  improve engine efficiency but can also cause unwanted combustion events. The most common is 'backfire' - premature ignition of the  $H_2$ -air mixture during the intake stroke, leading to combustion in the intake system and possible failure. Preventing early ignition requires eliminating ignition sources such as hot spark plug electrodes and exhaust valves, and modifying the ICE. Keeping ignitable mixtures away from ignition sources is another way to prevent backfire. In this case, variable valve timing and carefully managed injection timing are used to prevent backfire by introducing a cooling period with fresh air and minimizing  $H_2$  during the initial intake phase [1, 60]. Pre-ignition can also occur when the inlet valves are closed and the charge is compressed, resulting in extremely high pressures and potential damage. Ultimately, self-ignition (knock) of the unburned mixture can occur, as in any SI ICE. In an  $H_2$  ICE, knock is less likely than in gasoline engines, but its effects may be more severe due to the high burning speed of  $H_2$  mixtures.

$H_2$  PFI has been applied in various demonstration vehicles, either modified from existing models or purpose-built for  $H_2$ . Modifications for  $H_2$  operation focus on the fuel system (from storage to injection) and engine control unit programming. Quantum Tecstar converted over 30 vehicles for  $H_2$ , using the Toyota Prius hybrid as a base. Two compressed  $H_2$  tanks replace the gasoline tank, preserving the vehicle's interior. The Prius engine is turbocharged to boost  $H_2$  performance. The Quantum  $H_2$  Prius offers similar drivability to the gasoline version, with a range of 100–130 km and compliance with SULEV II emissions standards [121].

Designing a dedicated  $H_2$  vehicle required additional hardware considerations [125].

Shinde and Karunamurthy [97] observed that current PFI and DI  $H_2$  ICEs provide favorable brake thermal efficiency compared to gasoline ICEs.  $H_2$  properties are better suited for gasoline-type engines, but specific adjustments are needed to utilize  $H_2$ 's potential fully. For DI, a late injection strategy is recommended for optimal combustion. Efficiency losses must be minimized. EGR increases ICE efficiency, and further dehumidifying EGR improves it; thus, arrangements for EGR dehumidification are suggested. Downsizing the engine increases efficiency but also raises  $NO_x$  emissions, requiring a balance between  $NO_x$  and efficiency. Research should focus on hybrid fueling systems combining DI and PFI to enhance efficiency and lower emissions.

$H_2$ -fueled ICEs have demonstrated higher-brake thermal efficiency than those using fossil fuels. However, irregular combustion such as backfiring in  $H_2$ -injected engines, limits performance improvements due to  $H_2$ 's low ignition energy and high flame speed. Volumetric efficiency drops significantly during backfire, and damage to intake and fuel injection systems can occur. Backfire is triggered by residual

exhaust gas at high temperatures, hot spots, and irregular spark plug discharge, which promote pre-ignition of the H<sub>2</sub>-air mixture. Gao et al. [32] analyzed factors leading to backfire, including incorrect valve and injection timing and high A/F ratios, and reviewed backfire control methods, discussing their pros and cons. The main causes are excessive residual exhaust gas, slow combustion, and uneven H<sub>2</sub> distribution near intake valve seats. Backfire control strategies require specific conditions to remain effective; outside these, they may negatively impact results. Power loss is almost unavoidable for naturally aspirated ICEs when backfire prevention is implemented. Various strategies are recommended to mitigate performance loss, and multi-objective optimization is proposed to achieve the best overall efficiency.

BMW created the H<sub>2</sub> 7 car with a dual-fuel system that allows for operation on either H<sub>2</sub> or gasoline. In H<sub>2</sub> mode, it uses a variable A/F ratio lean-burn strategy for low and medium loads, and a throttled stoichiometric approach for high loads. Approximately 8 kg of H<sub>2</sub> are stored in a cryogenic tank in the trunk, providing a range of 200 km. Emission tests of a mono-fuel H<sub>2</sub> 7 variant showed very low emissions. Using a special after-treatment system with two catalysts (one for stoichiometric and one for minimizing NO<sub>x</sub> spikes during transitions), the car achieved drive-cycle NO<sub>x</sub> emissions of 0.0008 g/mi, just 3.9% of the SULEV II threshold [43].

Vogel [124] developed a large diesel engine with H<sub>2</sub> DI into the combustion chamber, achieving high power density and reduced exhaust emissions. Combustion occurred via self-ignition, following the diesel principle, with H<sub>2</sub> as the energy source, allowing CO<sub>2</sub>-free operation.

Prechtl and Dorer [83] reported that H<sub>2</sub>'s properties and use in high-power, large-displacement engines led to the concept of an engine with internal mixture formation and CI. A system developed by MAN B&W used electro-hydraulic control for injection. H<sub>2</sub> was injected at high pressure in gaseous form, with experiments and 3D flow simulations performed. The ignition process was modelled in 1D chemical simulations. Combustion in a diesel ICE is feasible, and the mixing system is key for effective H<sub>2</sub> combustion in large diesel ICEs.

Rottengruber et al. [88] performed studies on a DI H<sub>2</sub>-powered diesel engine, injecting H<sub>2</sub> at high pressure near top dead center and igniting by self-ignition. This was systematically tested on a single-cylinder engine. Combustion was analyzed using custom software to generate pressure curves and engine mechanics, and a computational model was developed to predict NO<sub>x</sub> emissions.

Some researchers have investigated various H<sub>2</sub>-fueled engines (see Table 1).

Brzeżański and Rodak [15] conducted theoretical and experimental work on a Kipor 186F SI ICE modified for H<sub>2</sub>. The engine utilized an H<sub>2</sub> DI system in the combustion chamber, enabling the regulation of heat release rate. H<sub>2</sub> DI, compared to inlet channel injection, greatly expanded the engine's operational range and prevented knocking. The right DI approach enabled combustion with a lower excess air coefficient, approaching stoichiometric conditions. This increased maximum cylinder pressure and improved engine

parameters, with no resultant knocking. The DI approach, employed during both the compression and combustion phases, enables H<sub>2</sub> to replace hydrocarbon fuels in ICEs fully.

Brzeżański and Rodak [16] also analyzed NO<sub>x</sub> formation during H<sub>2</sub>-air combustion in an SI ICE. They developed a strategy for generating and combusting H<sub>2</sub>-air mixtures, ensuring low NO<sub>x</sub>. This approach limits the N and O<sub>2</sub> reaction during operation. Preliminary tests have shown that this injection strategy enables progress monitoring. Unlike previous H<sub>2</sub> supply systems, this method allowed stoichiometric combustion without anomalies or auto-ignition. Monitoring the heat release rate and in-cylinder pressure rise was also possible. These engine parameters strongly influenced burning characteristics and NO<sub>x</sub> emissions. The developed system avoided knocking and allowed full NO<sub>x</sub> emission monitoring. Burning progress and NO<sub>x</sub> propensity can be evaluated by average pressure rise. Tests over a wide H<sub>2</sub>-air mixture range ( $\lambda = 2.03\text{--}1.05$ ) showed that NO<sub>x</sub> generation depends more on temporary pressure rise (and thus temperature) than O<sub>2</sub> availability. The H<sub>2</sub> injection strategy, which allows injection during either the compression or both compression and combustion phases, depending on the operating point, significantly influences operating parameters and NO<sub>x</sub> emissions, and could inform regulatory guidance.

Szlachetka et al. [109] simulated a gaseous fuel delivery system in a Wankel engine using a zero-dimensional model of the injector set, with gaseous H<sub>2</sub> injected into the RX 50 Wankel engine's intake manifold. The study was conducted at 3700 rpm and an inlet pressure of 0.4 MPa. Pressure time profiles in the fuel pipe and injector-to-intake tubing were analyzed. Maximum pressure fluctuations in the fuel rail reached 0.016 MPa at injector closure. Notable changes in fuel flow in the pipe to the intake manifold were observed, up to 0.002 kg/s. The maximum average injector mass flow was 0.00325 kg/s.

Mitianiec [69] noted that Wankel engines may be attractive in automotive applications due to their small size, compactness, simple design, smooth operation, and reduced vibration resulting from inertia forces. The main drawback is significant pollution (HCs, CO) and high BSFC, which can be addressed by H<sub>2</sub> DI and, in aviation, by using high-octane fuel in DI systems. The researcher simulated thermodynamic processes during scavenging, utilizing engine geometry, initial and boundary conditions to compute pressure, temperature, density, heat exchange, and volume as a function of piston angle in a zero-dimensional model. Mixture formation during compression-phase injection provided insights into air excess ratio. The model can be used for various fuels. Using H<sub>2</sub> lowers emissions but also reduces efficiency.

The author concluded that:

1. While the inlet port is opened, only a brief moment is available to fill the chamber with fresh air. Emission discharge continues longer due to high pressure, depending on the outlet port area. Rotor contact points should be minimized for effective sealing.

2. For naturally aspirated rotary Wankel engines, volumetric efficiency remains below 1.0 due to emissions that hinder air flow into the chamber.
3. Fuel injection must occur during the compression phase to minimize fuel waste.
4. A gasoline-homogeneous mixture engine produces more internal work (and power) than an H<sub>2</sub> engine, due to gasoline's higher caloric value under the same settings.
5. The mass of charge in the naturally aspirated Wankel engine varies slightly with engine speeds.
6. Exhaust pressure within the port is largely unaffected by the fuel at the speed.
7. The engine achieves peak power at high speeds, specifically 12,000 rpm in this case.
8. To achieve high overall efficiency, a DI fuel layout is needed for stratified charge.
9. The scavenging process is crucial for ported engines.

Szwaja [110] studied knocking in an H<sub>2</sub>-powered engine. Knocking intensity was defined as in-cylinder pressure fluctuations (sampled at 100 kHz) and processed with high-pass filtering (cutoff at 3.5 kHz). The study used a CFR engine with variable CR (6–14). A sharp rise in pressure pulsation amplitude was observed as CR rose from 11 to 12, attributed to auto-ignition of the H<sub>2</sub>-air mixture at the end of SI-controlled combustion. The dual nature of H<sub>2</sub> knock combustion was proposed. Pressure pulsation intensity during regular combustion (without H<sub>2</sub> auto-ignition) showed an exponential relationship with CR, directly related to the temperature of the H<sub>2</sub>-air mixture at ignition.

Kovar et al. [55] evaluated H<sub>2</sub>-fueled engines, focusing on mixture formation, combustion of air-H<sub>2</sub> mixtures with varying A/F ratios, NO<sub>x</sub> emissions, and power characteristics. Studies were conducted on a single-cylinder test engine (naturally aspirated and supercharged) and a six-cylinder turbocharged engine. Main technical challenges in H<sub>2</sub> engine development are (i) reduced power due to lower volumetric energy density of H<sub>2</sub>/air mixtures, and (ii) issues like backfire and early ignition. Engine concepts like turbocharging, intercooling, and internal blending with A/F equivalence ratio  $\Phi < 0.5$  can increase efficiency while keeping NO<sub>x</sub> low. The safest H<sub>2</sub>-powered engine system utilizes an in-cylinder fuel mixer, where air is drawn in first, followed by H<sub>2</sub> DI into the cylinder. No backfire was observed in lab tests (even when H<sub>2</sub> was introduced before inlet valve closure at  $\sim 1$  MPa).

Szajwajca et al. [111] examined a two-stage passive H<sub>2</sub> combustion setup for knock studies under various conditions. Experiments with a single-cylinder AVL 5804 engine assessed the effect of center of combustion (CoC) and excess A/F ratio ( $\lambda$ ) on knocking and its metrics. Tests at 1500 rpm, with CoC (2–18°CA aTDC) and  $\lambda = 1.25$ –2.0, showed strong knock at  $\lambda = 1.25$ –1.5, requiring higher  $\lambda$  to suppress it. Knocking depended more on  $\lambda$  than on CoC.

Lee et al. [57] studied H<sub>2</sub> DI, assessing three mixing methods: homogeneous, lean homogeneous, and lean-stratified in a single-cylinder ICE. Results show that H<sub>2</sub>'s significant heat loss requires delaying combustion. The lean-stratified charge (LSC) mode, designed to reduce high-temperature zones near the cylinder wall, achieved the highest BTE (34.09%) at low loads. However, this also

increased NO<sub>x</sub> emissions, illustrating the trade-off between efficiency and emissions in H<sub>2</sub> DI systems.

Bao et al. [11] tested a 2.0L turbocharged H<sub>2</sub> DI ICE, achieving 120 kW at 4400 rpm and 340 N·m at 2000 rpm. Peak BTE was 42.6% with a mildly lean A/F ratio ( $\lambda = 1.91$ ) at 2000 rpm. NO<sub>x</sub> emissions dropped by over 99.5% at speeds below 2000 rpm and by about 90% at 4400 rpm, with two-thirds of cases achieving NO<sub>x</sub> below 20 ppm using an NH<sub>3</sub>-SCR after-treatment system. This confirms that H<sub>2</sub> DI ICEs can deliver high power, efficiency, and near-zero emissions.

Wróbel et al. [132] reviewed advances in H<sub>2</sub> combustion vehicle technology, highlighting prototypes and summarizing key features (see Table 2). Since H<sub>2</sub> engine drivelines are mechanically similar to conventional ones, they are ideal for operators in challenging environments or those seeking stable maintenance costs. H<sub>2</sub> engine development is promising for applications that do not require dense refueling infrastructure. H<sub>2</sub> combustion vehicles tolerate varying H<sub>2</sub> quality, operate in harsh conditions, are reliable and user-friendly, and are mature, tested technology that ensures independence from rare earth metals. The main drawback is NO<sub>x</sub> emissions, requiring exhaust treatment.

According to [87], just a year after its prototype was revealed in October 2021, HYVIA presented the H<sub>2</sub>-powered Renault Master Van H2-TECH at the Paris Motor Show 2022. Its main advantages are zero emissions, a 5-minute refueling time, and a 400 km range. The Master Van H2-TECH is a spacious van with 12 m<sup>3</sup> cargo capacity, a 30 kW FC, a 33 kWh battery, and tanks for 6.4 kg of H<sub>2</sub>.

Various strategies are employed to enhance H<sub>2</sub> combustion and ICE efficiency while minimizing harmful emissions, including optimized A/F ratios, sophisticated injection systems, and EGR. These methods aim to enhance combustion efficiency, reduce NO<sub>x</sub> emissions, and minimize the production of other pollutants [34, 77, 104].

Optimized combustion can be realized via:

- Control of the air-fuel mixture is essential, as accurate management of this ratio is crucial. Operating the engine in a "fuel-lean" mode (with surplus air) can enhance efficiency. The rapid flame speed of H<sub>2</sub> enables stable combustion, even under lean conditions [6, 31, 50, 70, 84, 133].
- Injection techniques, particularly high-pressure DI systems, provide enhanced control over the timing of combustion and fuel distribution, resulting in improved efficiency and performance [34, 99].
- Stratified combustion, which employs stratified or spark-assisted diffusive combustion, can enhance combustion features and improve thermal efficiency [34].
- The timing of ignition, as sophisticated ignition systems can be employed to enhance the timing of combustion, ensures it occurs at the most efficient moment within the engine cycle [7, 34, 137].

Emission control can be realized via:

- EGR lowers combustion temperatures, which aids in reducing the creation of NO<sub>x</sub> [3, 34, 50, 77].
- Catalytic converters, because although hydrogen burning mainly generates water. Catalytic converters can also minimize NO<sub>x</sub> emissions [34, 104, 113, 117].

Table 1. Selected combustion engines supplied with H<sub>2</sub>

Refs	Type of engine	Combustion system	Bore × stroke [mm]	Displacement [dm <sup>3</sup> ]	CR [-]	Power output [kW]/speed [rpm]
[15, 16]	Kipor 186F, Single-cylinder, vertical 4-stroke, forced air cooled diesel	Single-cylinder, vertical 4-stroke, forced air cooled diesel. DI system. Modified by Heron chamber in the piston for a strong swirl during compression.	86 × 70	0.406	Original 19.3, after modification of burning space 15.1	Continuous 6.6, Maximum 7.4/3600
[110]	CFR Waukesha Single cylinder SI 4- 4-stroke water cooling		8.26 × 11.43	0.611	4.5–18.5	
[55]	OKC-Octane Single cylinder SI 4-stroke both naturally aspirated and supercharged	gas DI		0.61	8:1	
[55]	LIAZ ML637ENE 6-cylinder SI 4-stroke turbocharged		130 × 150	11.946	12:1	160/2000
[111]	AVL 5804 1-cyl., 4-valve, SI, TJI, supercharged	H <sub>2</sub> supplied from cylinder to main chamber at 6.5 bar. Two tanks in series before injector to reduce pressure pulsation.	85 × 90	0.5107	14.5:1	
[57]	Single-cylinder SG-DISI	Highly pressurized H <sub>2</sub> injected from three cylindrical vessels via modified piezo-actuated gasoline injector, with fire arrester and H <sub>2</sub> detector.	85 × 88			
[11]	4-stroke, DI H <sub>2</sub> -fueled			1		

Table 2. Selected prototype cars with H<sub>2</sub>-fuelled ICEs (based on [132])

Model	Engine	H <sub>2</sub> Tank	Range (km)
Ford P2000 (2001)	ICE 2.0 l straight-four engine Zetec (port injection)	Compressed (87 dm <sup>3</sup> , 250 bar, 1.5 kg)	100
Ford Shuttle Bus (2004)	ICE 6.8 l V10 Triton	Compressed (350 bar, 29.6 kg)*	240–320
ETEC Chevrolet Silverado (2004)	ICE 6.0 l V8	Compressed (3 × 150 dm <sup>3</sup> , 350 bar, 10.5 kg)*	230–260
Toyota Quantum Prius (2005)	ICE 1.4 l straight-four engine (electronic multi point H <sub>2</sub> injection)	Compressed (1.6 kg)	100–130
Toyota Corolla (racing vehicle) (2021)	ICE 1.6 l 3-cylinder turbo with intercooler	Compressed	
Lexus RC F designed vehicle (2022)	ICE 5.0 l V8		

\* Note: The higher brake specific fuel consumption BSFC is due to the relatively larger size and ~~ear~~ weight of these vehicles.

- Lean burn approaches, which involve operating the engine in a lean manner, enhance efficiency and decrease the release of specific emissions [4, 26]. Modifications to the engine can be focused on [7, 77, 85];
- Material enhancements, as the combustion of H<sub>2</sub> can be detrimental to engine parts. Changes such as reinforced valves and seats, upgraded connecting rods, and altered inlet manifolds are frequently required.
- Elevated voltage ignition, as H<sub>2</sub> needs a more powerful spark to ignite. Therefore, ignition coils with higher voltage might be needed.

- The injectors' design, as they are meant for gaseous fuels, is essential for the efficient delivery of H<sub>2</sub>. Additional considerations specific to H<sub>2</sub> include [33, 62, 104, 108, 112]:
- Lubrication plays a crucial role in engines supplied with H<sub>2</sub>, as the low lubricity of H<sub>2</sub> can create difficulties. A careful choice of lubricating oils, along with possibly other additives, may be necessary.
- Combustion instabilities, as in H<sub>2</sub> burning, may be susceptible to them. Sophisticated control methods are necessary to ensure consistent and reliable performance.
- H<sub>2</sub> embrittlement, as H<sub>2</sub> may induce it in specific metals. The selection of materials and the design of the engine need to consider this. Improvements in performance can be reached via:
- Turbocharging and supercharging, which can enhance the volume of air drawn into the ICE, boosting power production [23, 34, 99, 135].
- Dual-fuel operation realized by combining H<sub>2</sub> with fuels, like NG to rise efficiency and lower emissions [10, 99].
- Incorporation of nanomaterials into H<sub>2</sub> to enhance thermal conductivity and heat transfer [81].

#### 4. Vehicles with fuel cells (FCs)

Pramuanjaroenkij and Kakaç [82] reported that H<sub>2</sub> can be supplied to fuel cells (FCs) to generate electricity for powering vehicles, resulting in zero greenhouse gas emissions and requiring no direct combustion.

FCs serve as energy-conservation technologies for the 21st century, applicable to mobile, stationary, and especially FC electric vehicles (FCEVs), which are classified as zero-emission vehicles. H<sub>2</sub> FC vehicles, which use hydrogen as a power source, are also referred to as hydrogen electric vehicles or FC electric vehicles. Many individuals mistakenly thought that FCs were batteries; however, FCs

can continuously generate electric power as long as they receive a constant fuel supply. Batteries can supply electrical energy only as long as their stored charge permits; once depleted, they provide no further energy. FCs have been utilized in various applications, including unmanned aerial vehicles (UAVs), unmanned underwater vehicles (UUVs), as well as automobiles, trucks, and buses. Over the past five years, research on FCs has focused on catalysts and membranes, fluid flow fields, motors and converters in FC vehicles, sensors and controls, cooling methods for FCs, machine learning applications, modeling, simulations of FC vehicles, and especially energy management systems within these vehicles.

As noted in [41], the path to widespread acceptance of hydrogen fuel cell vehicles (HFCVs) is fraught with challenges. Central to these issues are the substantial costs associated with vehicle manufacturing and H<sub>2</sub> FC technology, insufficient refueling infrastructure, and concerns regarding the efficiency and environmental impact of H<sub>2</sub> generation. Despite these challenges, technological advancements, economies of scale, and significant investments in research and development (R&D) could help overcome these barriers.

Stakeholder involvement is essential for advancing HFCVs. Car manufacturers such as Toyota, Hyundai, Honda, and Mercedes-Benz are continuously improving their HFCV models, demonstrating strong commitment to this technology. However, a broader transition to HFCVs requires a more comprehensive set of actions and collaborations, including public education initiatives, development of H<sub>2</sub> infrastructure, and funding for research to improve the cost and efficiency of HFCVs.

Government initiatives and policies also play a significant role in the adoption of HFCVs. Governments can promote the development of HFCVs through financial incentives, infrastructure development, clear regulations and standards, and public awareness campaigns. Governments must integrate HFCVs into their broader energy, environment, and economic strategies to ensure balance and consistency. The advancement of HFCVs is closely linked to the broader expansion of the hydrogen economy.

Fang et al. [28] evaluated the current status of fuel-cell electric vehicles (FC-EVs), ongoing research, and the associated challenges and opportunities. Proton-exchange membrane fuel cells (PEMFCs) and solid oxide fuel cells (SOFCs) face significant obstacles to widespread adoption. PEMFC vehicles are challenged mainly by high costs, limited durability, and infrastructure gaps. The reliance on expensive platinum-based catalysts increases production costs, while degradation from catalyst poisoning and membrane failure affects long-term viability. Additionally, the lack of H<sub>2</sub> refueling stations is a significant barrier to the adoption of PEMFC vehicles.

In contrast, SOFCs do not require costly platinum group catalysts; however, SOFC vehicles face challenges related to high operating temperatures, fuel flexibility, system complexity, and stack degradation. Operating at 500–1000°C, SOFCs encounter issues with thermal management and material compatibility. Ensuring efficient operation with various fuel types, optimizing system design, and minimizing stack degradation are crucial for advancing

SOFC technology. Collaborative R&D efforts are crucial for addressing these challenges and accelerating the adoption of both PEMFC and SOFC vehicles as sustainable transportation solutions.

Günaydin et al. [37] compared passenger and commercial H<sub>2</sub> FC vehicles with internal combustion engine (ICE) cars, plug-in hybrid electric vehicles, and battery electric vehicles, focusing on well-to-wheel efficiency, range, fuel consumption, refueling/recharging time, emissions, and vehicle costs. They found that while battery electric vehicles (BEVs) lead the passenger vehicle market due to lower costs and expanding infrastructure, HFCVs are well-suited for commercial vehicles, offering fast refueling and long range. The transition to HFCVs faces hurdles, including limited infrastructure compared to gasoline and electric systems, as well as the higher cost of hydrogen production relative to gasoline and electricity, both of which must be addressed for widespread adoption. The increasing use of renewable energy may reduce electricity costs for electrolysis, thereby lowering overall hydrogen production costs and facilitating the generation of green hydrogen. Recent years have seen significant growth in hydrogen infrastructure and electrolysis capacity worldwide, particularly in Asia-Pacific countries. Enhanced government incentives and investments, along with financial support for consumers and manufacturers, are vital for increasing HFCV adoption. Additionally, R&D efforts are crucial for advancing hydrogen infrastructure and production technologies.

Baba et al. [8] examined the use of FCs and energy management in hybrid vehicles. FC vehicles offer significant advantages over battery-electric vehicles in terms of range, energy efficiency, charging time, and adaptability to different climates. The classification and a brief overview of HEVs/FCs are provided, followed by a summary of FC HEVs that illustrate various hybrid vehicle configurations.

### Topological categorization

Hybridization refers to the integration of two energy sources and one propulsion type, or two types of propulsion. In HEVs, this means combining electric and thermal propulsion. In FCEVs, the system starts with the battery supplying energy to the DC bus [63]. The DCU maintains steady bus voltage and delivers propulsion energy to the motor drive converter. The DC/AC converter controls motor speed and torque, and the motors convert electrical energy into kinetic energy [80].

- 1) Complete FCEV framework: The FC stack serves as the sole energy source, comprising a DC-DC converter, fuel tank, FC stack, inverter, and electric motor [40], which provides high efficiency, a simple design, system reliability, and a user-friendly driving experience [40].
- 2) FC + Battery integration: This design includes a unidirectional DC-DC converter (UDC) connected to the storage system and an inverter directly linked to the motor. The storage system provides the high current needed for engine startup [40, 91].
- 3) FC + Ultracapacitor (UC) hybridization: This configuration utilizes an ultracapacitor to extend the life of the storage system, but its low energy density limits its application to short-term use [90].

- 4) FC + (Battery + UC) hybridization: This setup includes an FC connected to the DC bus, with two DC-DC converters (one unidirectional and one bidirectional) located between the FC and the capacitor [80, 90].
- 5) FC + battery + PV hybridization: A hybrid system combining FC, battery, and photovoltaic (PV) sources, with the storage system linked to the DC bus via a bidirectional converter. PV power depends on solar radiation and temperature [73].

Such topologies were presented in Fig. 1.

According to Voelckner [123], since 2015, three H<sub>2</sub>-fueled vehicles have been available for purchase from major automakers: the Honda Clarity FC, Hyundai Nexo SUV, and Toyota Mirai. However, Honda has discontinued all Clarity models. Hyundai has sold only about 1600 Nexo SUVs in six years, and Toyota has sold approximately 14,300 Mirai sedans in the U.S. over two generations, sometimes relying on substantial discounts to boost sales. In 2025, Honda will launch the CR-Ve: FCEV, an improved compact crossover with a hydrogen FC (co-developed with GM) and a larger battery for plug-in charging, offering 29 miles of electric range and 241 miles from the FC. It will be available for lease in California only, with an expected annual volume of 300 vehicles.

According to [127], there are two main types of pure electric vehicles using FCs as their primary electricity source: FC electric vehicles (FCEVs) and FC hybrid electric vehicles (FCHEVs). The primary challenges in FC electric mobility include low FC efficiency, cold start issues, difficulties with hydrogen storage, the need for cost reduction, safety risks, and traction system problems.

Waseem et al. [128] noted that energy storage for electric vehicles can be achieved using various technologies, including lithium-ion batteries (LIBs), lead-acid batteries (LABs), solid-state batteries (SSBs), FCs, and ultracapacitors (UCs).

Samuel et al. [92] analyzed a hydrogen FC vehicle based on the Toyota Mirai and confirmed its fuel efficiency using real-world test data. This validated model was used to calculate fuel efficiency for actual driving cycles recorded in Mexico City in 2019, encompassing three distinct drive cycles that accurately reflect real urban driving conditions.

On February 28, 2024, at the 16th Expo Foro Movilidad in Mexico, FOTON unveiled the HC12 hydrogen fuel cell bus, the first hydrogen FC bus in Mexico. The HC12 features a 120 kW fuel cell engine and a 35 MPa hydrogen system, offering a range of up to 550 km (400 km from hydrogen, 150 km from electricity). It is emission-free, environmentally adaptable, highly safe, and fuel-efficient, making it ideal for medium- to long-distance transport, luxury tourism, and group services [30].

Thanks to hydrogen technology and larger, lightweight hydrogen tanks totaling 51.2 kg, the Solaris Urbino 18 H<sub>2</sub> bus excels on long routes. The BALLARD FCmove HD+ FCs, rated at 100 kW, achieve 57% efficiency and can operate for over 30,000 hours between -25°C and +50°C. The bus is powered by a 240 kW motor, delivering 1470 Nm of continuous torque and 2100 Nm peak torque [100]. Such buses have been tested in Brasov, Romania, and can be refueled in 5–10 minutes, offering a range of around 350

km. The cost is approximately EUR 700,000, which is about EUR 100,000 more than the electric model. The Solaris hydrogen bus has also been tested in Cluj-Napoca and Târgu Mureş [46].

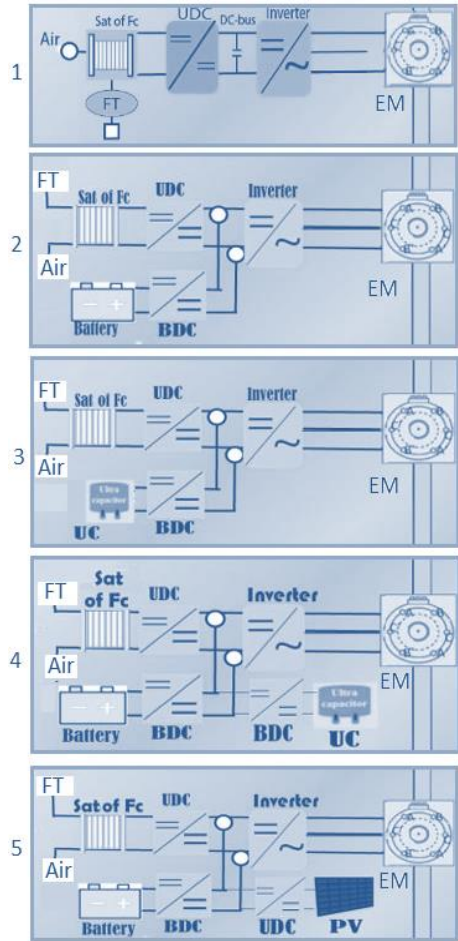


Fig. 1. Topologies of vehicles with fuel cells (FCs): 1 – The complete FCEV framework, 2 – The FC design + Battery integration, 3 – The FC arrangement + UC hybridization, 4 – The FC + (Battery + UC hybridization) set, 5 – The FC arrangement + Battery + PV hybridization arrangement

Currently, two major technical challenges for H<sub>2</sub> FCs are the high cost of catalysts and the frequent replacement of membrane materials that do not meet durability requirements [136]. According to [20], dynamic loading and FC costs are the main barriers to the successful commercialization of FCEVs and FCHEVs.

Issues related to hydrogen transportation can be addressed with innovative storage materials that are lightweight, strong, cost-effective, and suitable for long-distance, high-capacity delivery. For example, Zhang Jinying's team at Xi'an Jiaotong University utilized graphene for hydrogen storage, addressing challenges related to storage and transport. By using NaH or LiH as raw materials and controlling the encapsulation area of graphene, they achieved stable hydrogen release via interfacial nanovale control [56]. Using NaH or LiH as fuel allows for higher hydrogen storage density and is suitable for other gases as well. These materials offer strong chemical stability and mechanical strength, making them suitable for high-

temperature applications and emergency power for vehicles, drones, and semi-mobile devices [56].

Proton exchange membranes are essential for all types of H<sub>2</sub> FCs, but are very expensive. The widely used RSO<sub>3</sub>H (R = organic group) Nafion membrane, produced by DuPont, has a high cost and limited ion transport, which raises the price of H<sub>2</sub> FC vehicles. The catalysts used are also extremely expensive, costing twice as much as gold, further limiting the advancement of H<sub>2</sub> FCs [136].

Brzeżański et al. [17] conducted initial tests, approximately 2.5 hours in duration, on the Toyota Mirai FC powertrain in a thermoclimatic chamber at temperatures ranging from -10°C to -18°C, simulating winter conditions in temperate climates. They found that the operating principles and methods of the FC power unit differ significantly from those of combustion engines. Since climate conditions greatly affect FC performance, testing in a thermoclimatic chamber was necessary. During the tests, the drive system and electrical components were covered with condensed water, but no operational disruptions were observed.

Pielecha et al. [79] examined a Toyota Mirai model with a FC hybrid system (see Table 3), which shares many design features with hybrid cars. Innovative FC technologies were implemented, including compressed hydrogen tanks and advanced control systems. The study analyzed FC operation during ignition and driving, focusing on the hydrogen injection method of the three fuel injectors. The relationship between the FC and the high-voltage battery was also examined. It was demonstrated that increasing the electric motor's supply voltage at high torque levels results in a threefold voltage gain (up to approximately 650 V), doubling the drive system's torque compared to standard values.

Table 3. Toyota Mirai vehicle drive system characteristics [115]

Parameter		Value
Vehicle	mass	1850 kg
	maximum speed	179 km/h
Vehicle range	type approval cycle	approx. 550 km (NEDC test)
FC	type	PEM (polymer electrolyte)
	power	114 kW
	power density	2.0 kW/kg; 3.1 kW/dm <sup>3</sup>
	cell number	370
	humidification	internal circulation
Electric motor	type	synchronous AC
	maximum power	113 kW
	maximum torque	335 N·m
Battery	type	NiMH
H <sub>2</sub> storage	volume of tanks	front – 60 dm <sup>3</sup> , back – 62.4 dm <sup>3</sup>
	pressure/mass	70 MPa/5 kg H <sub>2</sub>
Refueling	time	3 min

Małek [61] reported that the method of supplying fuel to the FC cathode significantly affects the durability and efficiency of hydrogen energy conversion. FCs are inherently variable systems. The researchers studied a Nexa FC module (1.2 kW net output). To control the pump's airflow, a master-slave regulator was designed, featuring a sub-

regulator that works in conjunction with a brushless motor speed controller to adjust the airflow. A separate brushless motor was connected to the main regulator output. This approach allowed testing of different airflow regulation techniques independently of the initial controller's protocols. Airflow regulation of the PEM FC enabled identification and maintenance of the peak net power output of the FC stack, regardless of variations in controlled object parameters and external conditions. Adaptive extremum control with bi-factor assessment enabled automatic adjustment of controller parameters in response to changing system characteristics, improving both the value and speed of finding the optimum operating point.

While the development and market introduction of FC electric vehicles are progressing rapidly, several challenges remain for their practical application in vehicles, limiting the widespread adoption of FC technology in automotive powertrains. The main issues are [101]:

- Limited flexibility in power flow control in PEMFC + battery systems
- Significant power flow losses in PEMFC + battery + ultracapacitor configurations, complicating energy management
- Low battery power density results in larger, more expensive battery systems and increased vehicle mass.

## 5. Summary

Several mechanisms describing H<sub>2</sub> combustion have been developed recently, exhibiting varying degrees of complexity and accuracy. Further studies are needed to facilitate the incorporation of such mechanisms into AI-based modeling of H<sub>2</sub> combustion and control algorithms for real applications, including internal combustion engines (ICEs).

Future research might focus on increasing H<sub>2</sub> production from renewable sources, investigating novel materials or production techniques that reduce the costs of fuel cells (FCs) and H<sub>2</sub> generation, improving storage and distribution methods, and advancing materials science to lower FC costs. Additionally, it is crucial to perform a life-cycle assessment of hydrogen fuel cell vehicles (HFCVs), especially focusing on the recycling or disposal of proton exchange membrane (PEM) materials, the long-term environmental benefits and trade-offs, and the potential for partnerships among governments, industry stakeholders, and academia to address ongoing technical and economic challenges.

The growth of the market for H<sub>2</sub> internal combustion engine (H<sub>2</sub>ICE) vehicles heavily depends on advancements in H<sub>2</sub> infrastructure and the establishment of appropriate legal regulations. Further studies are needed for H<sub>2</sub> engines, particularly focusing on the development of exhaust gas treatment technologies to reduce NO<sub>x</sub> emissions. Fuel cell vehicles (FCVs) can reduce emissions and provide a clean energy alternative to gasoline-powered cars. However, their development depends on the availability of H<sub>2</sub> fuel and the expansion of refueling infrastructure.

## Nomenclature

A/F	air-fuel
BSFC	brake specific fuel consumption
CI	compression ignition
CNG	compressed natural gas
CR	compression ratio
DI	direct injection
FC	fuel cell

FI	fuel injection
HEV	hybrid electric vehicle
ICE	internal combustion engine
NG	natural gas
PFI	port fuel injection
SI	spark ignition

## Bibliography

[1] Abele AR. Quantum hydrogen storage systems, Sacramento, CA 2006.

[2] Ahmed SS, Mauß F, Moréac G, Zeuch T. A comprehensive and compact n-heptane oxidation model derived using chemical lumping. *Phys Chem Chem Phys.* 2007;9:1107-1126. <https://doi.org/10.1039/B614712G>

[3] Aldajah S, Ajayi OO, Fenske GR, Goldblatt IL. Effect of exhaust gas recirculation (EGR) contamination of diesel engine oil on wear. *Wear.* 2007;263:93-98. <https://doi.org/10.1016/j.wear.2006.12.055>

[4] Alrazen HA, Abu Talib AR, Adnan R, Ahmad KA. A review of the effect of hydrogen addition on the performance and emissions of the compression – Ignition engine. *Renew Sustain Energy Rev.* 2016;54:785-796. <https://doi.org/10.1016/j.rser.2015.10.088>

[5] Altinay G, Macdonald RG. Determination of the rate constant for the  $\text{OH}(\text{X}^2 \Pi) + \text{OH}(\text{X}^2 \Pi) \rightarrow \text{H}_2\text{O} + \text{O}(\text{^3 P})$  reaction over the temperature range 295 to 701 K. *J Phys Chem A.* 2014;118:38-54. <https://doi.org/10.1021/jp409344q>

[6] Aritra C, Suhail D, Bijan KM. Combustion performance and emission characteristics of hydrogen as an internal combustion engine fuel. *J Aeronaut Automot Eng JAAE.* 2014;1:1-6.

[7] Ayissi MZ, Newen IA, Alloune R, Bitondo D. Effects of gasoline and hydrogen blends on exhaust gas emissions and fuel consumption from gasoline internal combustion engines. *J Combust.* 2022;2022:1-10. <https://doi.org/10.1155/2022/5526205>

[8] Baba MA, Labbadi M, Cherkaoui M, Maaroufi M. Fuel cell electric vehicles: a review of current power electronic converters topologies and technical challenges. *IOP Conf Ser Earth Environ Sci.* 2021;785:012011. <https://doi.org/10.1088/1755-1315/785/1/012011>

[9] Bajerlein M, Bor M, Karpuk W, Smolec R, Spadło M. Strength analysis of critical components of high-pressure fuel pump with hypocycloid drive. *Bull Pol Acad Sci Tech Sci.* 2020;1341-1350. <https://doi.org/10.24425/bpasts.2020.135380>

[10] Bakar RA, Widudo, Kadrigama K, Ramasamy D, Yusaf T, Kamarulzaman MK et al. Experimental analysis on the performance, combustion/emission characteristics of a DI diesel engine using hydrogen in dual fuel mode. *Int J Hydrog Energy.* 2024;52:843-860. <https://doi.org/10.1016/j.ijhydene.2022.04.129>

[11] Bao L, Sun B, Luo Q, Li J, Qian D, Ma H et al. Development of a turbocharged direct-injection hydrogen engine to achieve clean, efficient, and high-power performance. *Fuel.* 2022;324:124713. <https://doi.org/10.1016/j.fuel.2022.124713>

[12] Bor M, Borowczyk T, Idzior M, Karpuk W, Smolec R. Analysis of hypocycloid drive application in a high-pressure fuel pump. *MATEC Web Conf.* 2017;118:00020. <https://doi.org/10.1051/matecconf/201711800020>

[13] Bor M, Borowczyk T, Karpuk W, Smolec R. Determination of the response time of new generation electromagnetic in- jectors as a function of fuel pressure using the internal photoelectric effect. 2018 Int. Interdiscip. PhD Workshop IIPHDW, Swinoujście: IEEE; 2018. <https://doi.org/10.1109/iiphdw.2018.8388385>

[14] Brzeżański M, Papuga T, Rodak Ł. Analysis of creation and combustion process of hydrogen-air mixtures by optical method in isochoric chamber. *Combustion Engines.* 2017;170:121-125. <https://doi.org/10.19206/CE-2017-320>

[15] Brzeżański M, Rodak Ł. Investigation of a new concept of hydrogen supply for a spark-ignition engine. *Combust Engines.* 2019;178:140-143. <https://doi.org/10.19206/CE-2019-324>

[16] Brzeżański M, Rodak Ł. Influence of the method of creating a hydrogen-air mixture on the emission of nitrogen oxides in a spark-ignition engine. *Combustion Engines.* 2019;178:224-227. <https://doi.org/10.19206/CE-2019-339>

[17] Brzeżański M, Szałek A, Szramowiat M. Tests of the vehicle's power unit with fuel cells at a reduced ambient temperature. *Combustion Engines.* 2019;179:65-69. <https://doi.org/10.19206/CE-2019-410>

[18] Burke MP, Chaos M, Ju Y, Dryer FL, Klippenstein SJ. Comprehensive  $\text{H}_2/\text{O}_2$  kinetic model for high-pressure combustion. *Int J Chem Kinet.* 2012;44:444-474. <https://doi.org/10.1002/kin.20603>

[19] Burke MP, Klippenstein SJ. Ephemeral collision complexes mediate chemically termolecular transformations that affect system chemistry. *Nat Chem.* 2017;9:1078-1082. <https://doi.org/10.1038/nchem.2842>

[20] Chandran M, Palanisamy K, Benson D, Sundaram S. A review on electric and fuel cell vehicle anatomy, technology evolution and policy drivers towards EVs and FCEVs market propagation. *Chem Rec.* 2022;22:e202100235. <https://doi.org/10.1002/tcr.202100235>

[21] Combustion Research Group. The San Diego Mechanism: chemical kinetic mechanisms for combustion applications. 2014.

[22] Dagaout P, Lecomte F, Mieritz J, Glarborg P. Experimental and kinetic modeling study of the effect of NO and  $\text{SO}_2$  on the oxidation of  $\text{CO}_2$  mixtures. *Int J Chem Kinet.* 2003;35:564-575. <https://doi.org/10.1002/kin.10154>

[23] Das LM. Hydrogen engines: design, performance evaluation, combustion analysis, and exhaust emissions. 1st ed. Newark: John Wiley & Sons, Incorporated; 2025.

[24] Daszkiewicz P, Kołodziejek D. Comparison and analysis of modern combustion powertrain systems of rail vehicles. *Combustion Engines.* 2024;196:46-53. <https://doi.org/10.19206/CE-171385>

[25] Davis SG, Joshi AV, Wang H, Egolfopoulos F. An optimized kinetic model of  $\text{H}_2/\text{CO}$  combustion. *Proc Combust Inst.* 2005;30:1283-1292. <https://doi.org/10.1016/j.proci.2004.08.252>

[26] Davy M, Evans RL, Mezo A. The ultra lean burn partially stratified charge natural gas engine. *SAE Technical Paper* 2009-24-0115. 2009. <https://doi.org/10.4271/2009-24-0115>

[27] Escalante Soberanis MA, Fernandez AM. A review on the technical adaptations for internal combustion engines to operate with gas/hydrogen mixtures. *Int J Hydrol Energy*. 2010;35:12134-12140. <https://doi.org/10.1016/j.ijhydene.2009.09.070>

[28] Fang T, Vairin C, Von Jouanne A, Agamloh E, Yokochi A. Review of fuel-cell electric vehicles. *Energies*. 2024;17: 2160. <https://doi.org/10.3390/en17092160>

[29] Fiore M, Magi V, Viggiano A. Internal combustion engines powered by syngas: a review. *Appl Energy*. 2020;276: 115415. <https://doi.org/10.1016/j.apenergy.2020.115415>

[30] FotonMotor. The first hydrogen fuel cell bus in Mexico originated from Foton 2024. <https://www.fotonmotor.com/newsDetaila799d935.html>

[31] Fu Z, Li Y, Wu W, Li Y, Gao W. Experimental study on the combustion and emission performance of the hydrogen direct injection engine. *Int J Hydrol Energy*. 2024;61:1047-1059. <https://doi.org/10.1016/j.ijhydene.2024.02.276>

[32] Gao J, Wang X, Song P, Tian G, Ma C. Review of the backfire occurrences and control strategies for port hydrogen injection internal combustion engines. *Fuel*. 2022;307:121553. <https://doi.org/10.1016/j.fuel.2021.121553>

[33] Gao N, Geng Z, Zhao W, Geng L, Dong F, Huang D. Review on the combustion and emission characteristics of hydrogen engine. *Int J Hydrol Energy*. 2025;143:121-146. <https://doi.org/10.1016/j.ijhydene.2025.05.321>

[34] Gao W, Fu Z, Li Y, Li Y, Zou J. Progress of performance, emission, and technical measures of hydrogen fuel internal-combustion engines. *Energies*. 2022;15:7401. <https://doi.org/10.3390/en15197401>

[35] Gharehghani A, Hosseini R, Mirsalim M, Yusaf TF. A computational study of operating range extension in a natural gas SI engine with the use of hydrogen. *Int J Hydrol Energy*. 2015;40:5966-5975. <https://doi.org/10.1016/j.ijhydene.2015.03.015>

[36] Gis M, Gis W. The current state and prospects for hydrogenisation of motor transport in Northwestern Europe and Poland. *Combustion Engines*. 2022;190(3):61-71. <https://doi.org/10.19206/CE-144560>

[37] Günaydin ÖF, Topcu S, Aksoy A. Hydrogen fuel cell vehicles: Overview and current status of hydrogen mobility. *Int J Hydrol Energy*. 2025;S0360319925004562. <https://doi.org/10.1016/j.ijhydene.2025.01.412>

[38] Habib MA, Abdulrahman GAQ, Alquaity ABS, Qasem NAA. Hydrogen combustion, production, and applications: A review. *Alex Eng J*. 2024;100:182-207. <https://doi.org/10.1016/j.aej.2024.05.030>

[39] Hagos FY, Aziz ARA, Sulaiman SA. Trends of syngas as a fuel in internal combustion engines. *Adv Mech Eng*. 2014; 6:401587. <https://doi.org/10.1155/2014/401587>

[40] Hames Y, Kaya K, Baltacioglu E, Turksoy A. Analysis of the control strategies for fuel saving in the hydrogen fuel cell vehicles. *Int J Hydrol Energy*. 2018;43:10810-10821. <https://doi.org/10.1016/j.ijhydene.2017.12.150>

[41] Hassan Q, Azzawi IDJ, Sameen AZ, Salman HM. Hydrogen fuel cell vehicles: opportunities and challenges. *Sustainability*. 2023;15:11501. <https://doi.org/10.3390/su151511501>

[42] Healy D, Kalitan DM, Aul CJ, Petersen EL, Bourque G, Curran HJ. Oxidation of C1–C5 alkane quaternary natural gas mixtures at high pressures. *Energy Fuels*. 2010;24:1521-1528. <https://doi.org/10.1021/ef9011005>

[43] Heller K, Ellgas S. Optimization of hydrogen internal combustion engine with cryogenic mixture formation. Graz, Austria: 2006, 49-58.

[44] Hong Z, Cook RD, Davidson DF, Hanson RK. A shock tube study of  $\text{OH} + \text{H}_2\text{O}_2 \rightarrow \text{H}_2\text{O} + \text{HO}_2$  and  $\text{H}_2\text{O}_2 + \text{M} \rightarrow 2\text{OH} + \text{M}$  using laser absorption of  $\text{H}_2\text{O}$  and  $\text{OH}$ . *J Phys Chem A*. 2010;114:5718-5727. <https://doi.org/10.1021/jp100204z>

[45] Hong Z, Davidson DF, Hanson RK. An improved H<sub>2</sub>/O<sub>2</sub> mechanism based on recent shock tube/laser absorption measurements. *Combust Flame*. 2011;158:633-644. <https://doi.org/10.1016/j.combustflame.2010.10.002>

[46] Hydrogen Central. Hydrogen bus tested on the streets of Romania 2021. <https://hydrogen-central.com/hydrogen-bus-romania/>

[47] Jasper AW, Kamarchik E, Miller JA, Klippenstein SJ. First-principles binary diffusion coefficients for H, H<sub>2</sub>, and four normal alkanes + N<sub>2</sub>. *J Chem Phys*. 2014;141:124313. <https://doi.org/10.1063/1.4896368>

[48] Jasper AW, Miller JA. Lennard-Jones parameters for combustion and chemical kinetics modeling from full-dimensional intermolecular potentials. *Combust Flame*. 2014;161:101-110. <https://doi.org/10.1016/j.combustflame.2013.08.004>

[49] Kéromnès A, Metcalfe WK, Heufer KA, Donohoe N, Das AK, Sung C-J et al. An experimental and detailed chemical kinetic modeling study of hydrogen and syngas mixture oxidation at elevated pressures. *Combust Flame*. 2013;160:995-1011. <https://doi.org/10.1016/j.combustflame.2013.01.001>

[50] Kim J, Chun KM, Song S, Baek H-K, Lee SW. The effects of hydrogen on the combustion, performance and emissions of a turbo gasoline direct-injection engine with exhaust gas recirculation. *Int J Hydrol Energy*. 2017;42:25074-25087. <https://doi.org/10.1016/j.ijhydene.2017.08.097>

[51] Klippenstein SJ. From theoretical reaction dynamics to chemical modeling of combustion. *Proc Combust Inst*. 2017; 36:77-111. <https://doi.org/10.1016/j.proci.2016.07.100>

[52] Konnov AA. Remaining uncertainties in the kinetic mechanism of hydrogen combustion. *Combust Flame*. 2008;152: 507-528. <https://doi.org/10.1016/j.combustflame.2007.10.024>

[53] Konnov AA. On the role of excited species in hydrogen combustion. *Combust Flame*. 2015;162:3755-3772. <https://doi.org/10.1016/j.combustflame.2015.07.014>

[54] Konnov AA. Yet another kinetic mechanism for hydrogen combustion. *Combust Flame*. 2019;203:14-22. <https://doi.org/10.1016/j.combustflame.2019.01.032>

[55] Kovar Z, Scholz C, Beroun S, Nydrle M, Drozda H, Blazek J et al. Hydrogen piston engines: R&D, experiences. *Combustion Engines*. 2006;125:28-36. <https://doi.org/10.19206/CE-117350>

[56] Lamb KE, Webb CJ. A quantitative review of slurries for hydrogen storage – slush hydrogen, and metal and chemical hydrides in carrier liquids. *J Alloys Compd*. 2022;906: 164235. <https://doi.org/10.1016/j.jallcom.2022.164235>

[57] Lee S, Kim G, Bae C. Effect of mixture formation mode on the combustion and emission characteristics in a hydrogen direct-injection engine under different load conditions. *Appl Therm Eng*. 2022;209:118276. <https://doi.org/10.1016/j.applthermaleng.2022.118276>

[58] Li J, Zhao Z, Kazakov A, Chaos M, Dryer FL, Scire JJ. A comprehensive kinetic mechanism for CO, CH<sub>2</sub>O, and CH<sub>3</sub> OH combustion. *Int J Chem Kinet*. 2007;39:109-136. <https://doi.org/10.1002/kin.20218>

[59] Li J, Zhao Z, Kazakov A, Dryer FL. An updated comprehensive kinetic model of hydrogen combustion. *Int J Chem Kinet*. 2004;36:566-575. <https://doi.org/10.1002/kin.20026>

[60] Liu X, Liu F, Zhou L, Sun B, Schock H. Backfire prediction in a manifold injection hydrogen internal combustion engine. *Int J Hydrol Energy*. 2008;33:3847-3855. <https://doi.org/10.1016/j.ijhydene.2008.04.051>

[61] Małek A. Adaptive search for a PEM fuel cell maximum net power. *Combustion Engines*. 2011;145:49-57. <https://doi.org/10.19206/CE-117101>

[62] Manigandan S, Ryu JI, Praveen Kumar TR, Elgendi M. Hydrogen and ammonia as a primary fuel – a critical review of production technologies, diesel engine applications, and challenges. *Fuel*. 2023;352:129100. <https://doi.org/10.1016/j.fuel.2023.129100>

[63] Marei MI, Lambert S, Pick R, Salama MMA. DC/DC converters for fuel cell powered hybrid electric vehicle. 2005 IEEE Veh. Power Propuls. Conf., Chicago, USA. 2005: 556-559. <https://doi.org/10.1109/VPPC.2005.1554614>

[64] Masood M, Mehdi SN, Ram Reddy P. Experimental investigations on a hydrogen-diesel dual fuel engine at different compression ratios. *J Eng Gas Turbines Power*. 2007;129: 572-578. <https://doi.org/10.1115/1.2227418>

[65] Matla J. Possible applications of prechambers in hydrogen internal combustion engines. *Combustion Engines*. 2022; 191(4):77-82. <https://doi.org/10.19206/CE-148170>

[66] Matla J, Kaźmierzak A, Haller P, Trocki M. Hydrogen as a fuel for spark ignition combustion engines – state of knowledge and concept. *Combustion Engines*. 2024;196:73-79. <https://doi.org/10.19206/CE-171541>

[67] Meisner J, Kästner J. Reaction rates and kinetic isotope effects of  $H_2 + OH \rightarrow H_2O + H$ . *J Chem Phys*. 2016;144: 174303. <https://doi.org/10.1063/1.4948319>

[68] Menes M. Program initiatives of public authorities in the field of hydrogenation of the economy in a global perspective, as of the end of 2020. *Combustion Engines*. 2022;189: 18-29. <https://doi.org/10.19206/CE-142170>

[69] Mitianiec W. Modelling and simulation of working processes in Wankel engine with direct hydrogen injection system. *Combustion Engines*. 2015;161:42-52. <https://doi.org/10.19206/CE-116890>

[70] Muraki H, Zhang G. Design of advanced automotive exhaust catalysts. *Catal Today*. 2000;63:337-345. [https://doi.org/10.1016/S0920-5861\(00\)00477-6](https://doi.org/10.1016/S0920-5861(00)00477-6)

[71] Musy F, Ortiz R, Ortiz I, Ortiz A. Hydrogen-fuelled internal combustion engines: direct injection versus port-fuel injection. *Int J Hydrog Energy*. 2024;S0360319924028106. <https://doi.org/10.1016/j.ijhydene.2024.07.136>

[72] Nguyen TL, Stanton JF. Ab Initio thermal rate calculations of  $HO + HO = O(^3 P) + H_2 O$  reaction and isotopologues. *J Phys Chem A*. 2013;117:2678-2686. <https://doi.org/10.1021/jp312246q>

[73] Nguyen V-L. Couplage des systèmes photovoltaïques et des véhicules électriques au réseau: problèmes et solutions. Université de Grenoble, 2014.

[74] Nieścioruk MJ, Bandrow P, Szufa S, Woźniak M, Siczek K. Biomass-based hydrogen extraction and accompanying hazards—review. *Molecules*. 2025;30:565. <https://doi.org/10.3390/molecules30030565>

[75] Ó Conaire M, Curran HJ, Simmie JM, Pitz WJ, Westbrook CK. A comprehensive modeling study of hydrogen oxidation. *Int J Chem Kinet*. 2004;36:603-622. <https://doi.org/10.1002/kin.20036>

[76] Olm C, Zsély IGy, Pálvölgyi R, Varga T, Nagy T, Curran HJ, et al. Comparison of the performance of several recent hydrogen combustion mechanisms. *Combust Flame*. 2014; 161:2219-2234. <https://doi.org/10.1016/j.combustflame.2014.03.006>

[77] Paluch M, Noga M. Influence of hydrogen addition on performance and ecological parameters of a spark-ignition internal combustion engine at part load typical for urban traffic. *Adv Sci Technol Res J*. 2025;19:262-270. <https://doi.org/10.12913/22998624/199738>

[78] Paykani A, Chehrmonavari H, Tsolakis A, Alger T, Northrop WF, Reitz RD. Synthesis gas as a fuel for internal combustion engines in transportation. *Prog Energy Combust Sci*. 2022;90:100995. <https://doi.org/10.1016/j.pecs.2022.100995>

[79] Pielecha I, Cieślik W, Szałek A. The use of electric drive in urban driving conditions using a hydrogen powered vehicle – Toyota Mirai. *Combustion Engines*. 2018;172:51-58. <https://doi.org/10.19206/CE-2018-106>

[80] Pires VF, Cordeiro A, Foito D, Silva JF. High step-up DC–DC converter for fuel cell vehicles based on merged quadratic boost–éuk. *IEEE Trans Veh Technol*. 2019;68:7521-7530. <https://doi.org/10.1109/TVT.2019.2921851>

[81] Polat F, Saridemir S, Gad MS, El-Shafay AS, Ağıbulut Ü. Enhancing diesel engine performance, combustion, and emissions reductions under the effect of cerium oxide nanoparticles with hydrogen addition to biodiesel fuel. *Int J Hydrog Energy*. 2024;83:884-896. <https://doi.org/10.1016/j.ijhydene.2024.08.031>

[82] Pramuanjaroenkit A, Kakaç S. The fuel cell electric vehicles: the highlight review. *Int J Hydrog Energy*. 2023;48: 9401-9425. <https://doi.org/10.1016/j.ijhydene.2022.11.103>

[83] Prechtl P, Dorer F. Wasserstoff-Dieselmotor mit Direkteinspritzung, hoher Leistungsdichte und geringer Abgasemission: Teil 2: Untersuchung der Gemischbildung, des Zünd- und des Verbrennungsverhaltens. *MTZ – Mot Z*. 1999;60: 830-837. <https://doi.org/10.1007/BF03226544>

[84] Premkartikkumar SR, Annamalai K, Pradeepkumar AR. Using hydrogen as a fuel in automotive engines – an investigation. *IJITR Int J Innov Technol Res*. 2013;1:90-93.

[85] Rameez PV, Mohamed Ibrahim M. A comprehensive review on the utilization of hydrogen in low temperature combustion strategies: combustion, performance and emission attributes. *J Energy Inst*. 2024;113:101511. <https://doi.org/10.1016/j.joei.2023.101511>

[86] Rasmussen CL, Hansen J, Marshall P, Glarborg P. Experimental measurements and kinetic modeling of  $CO/H_2/O_2/NO_x$  conversion at high pressure. *Int J Chem Kinet*. 2008; 40:454-480. <https://doi.org/10.1002/kin.20327>

[87] RenaultGroup. The Renault Master Van H2-Tech, a hydrogen-powered utility vehicle 2022. <https://www.renaultgroup.com/en/magazine/energy-and-motorization/everything-there-is-to-know-about-hydrogen-vehicles>

[88] Rottengruber H, Wiebicke U, Woschni G, Zeilinger K. Wasserstoff-Dieselmotor mit Direkteinspritzung, hoher Leistungsdichte und geringer Abgasemission: Teil 3: Versuche und Berechnungen am Motor. *MTZ – Mot Z*. 2000;61:122-128. <https://doi.org/10.1007/BF03226557>

[89] Rutkowska-Gorczyca MJ, Dziubek M, Wiśniewski M. Response of hydrogen charging diffusion of the austenitic stainless steel AISI 310s. *Combustion Engines*. 2024;198: 68-73. <https://doi.org/10.19206/CE-186591>

[90] Sadoun R. Intérêt d'une Source d'Energie Electrique Hybride pour véhicule électrique urbain– dimensionnement et tests de cyclage. Ecole Centrale de Lille, 2013.

[91] Sakka MA, Van Mierlo J, Gualous H, Lataire P. Comparison of 30KW DC/DC converter topologies interfaces for fuel cell in hybrid electric vehicle, Barcelona, Spain: 2009, p. 1–10.

[92] Samuel S, Gonzalez-Oropeza R, Cedillo Cornejo E. Hydrogen fuel cell vehicle for Mexico City. 2020. SAE Technical Paper 2020-01-1169. 2020. <https://doi.org/10.4271/2020-01-1169>

[93] Sangwan M, Krasnoperov LN. Disproportionation channel of self-reaction of hydroxyl radical,  $OH + OH \rightarrow H_2O + O$ ,

studied by time-resolved oxygen atom trapping. *J Phys Chem A.* 2012;116:11817-11822. <https://doi.org/10.1021/jp308885j>

[94] Saxena P, Williams FA. Testing a small detailed chemical-kinetic mechanism for the combustion of hydrogen and carbon monoxide. *Combust Flame.* 2006;145:316-323. <https://doi.org/10.1016/j.combustflame.2005.10.004>

[95] Shahpouri S, Gordon D, Hayduk C, Rezaei R, Koch CR, Shahbakti M. Hybrid emission and combustion modeling of hydrogen fueled engines. *Int J Hydrog Energy.* 2023;48: 24037-24053. <https://doi.org/10.1016/j.ijhydene.2023.03.153>

[96] Shi C, Ji C, Ge Y, Wang S, Yang J, Wang H. Effects of split direct-injected hydrogen strategies on combustion and emissions performance of a small-scale rotary engine. *Energy.* 2021;215:119124. <https://doi.org/10.1016/j.energy.2020.119124>

[97] Shinde BJ, K. K. Recent progress in hydrogen fuelled internal combustion engine (H2ICE) – a comprehensive outlook. *Mater Today Proc.* 2022;51:1568-1579. <https://doi.org/10.1016/j.matpr.2021.10.378>

[98] Sikora M, Orlinski P. Hydrotreated vegetable oil fuel within the Fit for 55 package. *Combustion Engines.* 2024;197(2):3-8. <https://doi.org/10.19206/CE-174554>

[99] Skobiej K. A review of hydrogen combustion and its impact on engine performance and emissions. *Combustion Engines.* 2025;200(1):64-70. <https://doi.org/10.19206/CE-195470>

[100] Solaris Bus & Coach. Solaris Urbino 18 hydrogen 2025. [https://www.solarisbus.com/public/assets/content/firma/onas/nowy\\_profil\\_firmy/Urbino\\_18\\_hydrogen\\_EN.pdf?\\_gl=1\\*\\_1ufe3y8\\*\\_up\\*MQ\\_\\*\\_ga\\*MTg1MjI5OTcxMy4xNzQ0NjMzNDc4\\*\\_ga\\_JKWEFR8KTK\\*MTc0NDYzMzQ3Ny4xLjAuMTc0NDYzMzQ3Ny4wLjAuMA](https://www.solarisbus.com/public/assets/content/firma/onas/nowy_profil_firmy/Urbino_18_hydrogen_EN.pdf?_gl=1*_1ufe3y8*_up*MQ_*_ga*MTg1MjI5OTcxMy4xNzQ0NjMzNDc4*_ga_JKWEFR8KTK*MTc0NDYzMzQ3Ny4xLjAuMTc0NDYzMzQ3Ny4wLjAuMA)

[101] Sorlei I-S, Bizon N, Thounthong P, Varlam M, Carcadea E, Culcer M et al. Fuel cell electric vehicles—a brief review of current topologies and energy management strategies. *Energies.* 2021;14:252. <https://doi.org/10.3390/en14010252>

[102] Starik AM, Titova NS, Sharipov AS, Kozlov VE. Syngas oxidation mechanism. *Combust Explos Shock Waves.* 2010; 46:491-506. <https://doi.org/10.1007/s10573-010-0065-x>

[103] Stępień Z. A comprehensive overview of hydrogen-fueled internal combustion engines: achievements and future challenges. *Energies.* 2021;14:6504. <https://doi.org/10.3390/en14206504>

[104] Stępień Z. Analysis of the prospects for hydrogen-fuelled internal combustion engines. *Combustion Engines.* 2024; 197(2):32-41. <https://doi.org/10.19206/CE-174794>

[105] Sun H, Yang SI, Jomaas G, Law CK. High-pressure laminar flame speeds and kinetic modeling of carbon monoxide/hydrogen combustion. *Proc Combust Inst.* 2007;31:439-446. <https://doi.org/10.1016/j.proci.2006.07.193>

[106] Sun P, Zhang Z, Chen J, Liu S, Zhang DH. Well converged quantum rate constants for the  $H_2 + OH \rightarrow H_2O + H$  reaction via transition state wave packet. *J Chem Phys.* 2018; 149:064303. <https://doi.org/10.1063/1.5046890>

[107] Sutherland JW, Patterson PM, Klemm RB. Rate constants for the reaction,  $O(3P)+H_2O \rightarrow OH+OH$ , over the temperature range 1053 K to 2033 K using two direct techniques. *Symp Int Combust.* 1991;23:51-57. [https://doi.org/10.1016/S0082-0784\(06\)80241-9](https://doi.org/10.1016/S0082-0784(06)80241-9)

[108] Szamrej G, Karczewski M. Exploring hydrogen-enriched fuels and the promise of HCNG in industrial dual-fuel engines. *Energies.* 2024;17:1525. <https://doi.org/10.3390/en17071525>

[109] Szlachetka M, Wendeker M, Czarnigowski J, Jakliński P, Grabowski Ł. A simulation research of a hydrogen injection system for a Wankel engine. *Combustion Engines.* 2010; 141:114-122. <https://doi.org/10.19206/CE-117153>

[110] Szwaja S. Hydrogen resistance to knock combustion in spark ignition internal combustion engines. *Combustion Engines.* 2011;144:13-19. <https://doi.org/10.19206/CE-117118>

[111] Szwajca F, Gawrysiak C, Pielecha I. Effects of passive pre-chamber jet ignition on knock combustion at hydrogen engine. *Combustion Engines.* 2024;198:110-122. <https://doi.org/10.19206/CE-189738>

[112] Taib NM, Abu Mansor MR, Wong WY. Hydrogen combustion in transportation and power generation. In: Su'ait MS, Jarimi H, Noor SAM, editors. *ACS Symp. Ser.*, 1499, Washington, DC: American Chemical Society; 2025:169-192. <https://doi.org/10.1021/bk-2025-1499.ch010>

[113] Teoh YH, How HG, Le TD, Nguyen HT, Loo DL, Rashid T et al. A review on production and implementation of hydrogen as a green fuel in internal combustion engines. *Fuel.* 2023;333:126525. <https://doi.org/10.1016/j.fuel.2022.126525>

[114] The CRECK Modelling Group. Hydrogen/CO Mech. Version 2012.

[115] Toyota Europe. Outline of the Mirai 2017. [www.toyota-europe.com](http://www.toyota-europe.com)

[116] University of California – Berkeley. GRI-Mech 3.0 1999.

[117] Ustolin F, Paltrinieri N, Berto F. Loss of integrity of hydrogen technologies: A critical review. *Int J Hydrog Energy.* 2020;45:23809-23840. <https://doi.org/10.1016/j.ijhydene.2020.06.021>

[118] Varga T, Nagy T, Olm C, Zsély IGy, Pálvölgyi R, Valkó É et al. Optimization of a hydrogen combustion mechanism using both direct and indirect measurements. *Proc Combust Inst.* 2015;35:589-596. <https://doi.org/10.1016/j.proci.2014.06.071>

[119] Varga T, Olm C, Nagy T, Zsély IGy, Valkó É, Pálvölgyi R et al. Development of a joint hydrogen and syngas combustion mechanism based on an optimization approach. *Int J Chem Kinet.* 2016;48:407-422. <https://doi.org/10.1002/kin.21006>

[120] Verhelst S, Demuynck J, Sierens R, Scarcelli R, Matthias NS, Wallner T. Update on the progress of hydrogen-fueled internal combustion engines. *Renew Hydrot Technol.* 2013; 381-400. <https://doi.org/10.1016/B978-0-444-56352-1.00016-7>

[121] Verhelst S, Wallner T. Hydrogen-fueled internal combustion engines. *Prog Energy Combust Sci.* 2009;35:490-527. <https://doi.org/10.1016/j.pecs.2009.08.001>

[122] Verhelst S, Wallner T, Eichlseder H, Naganuma K, Gerbig F, Boyer B et al. Electricity powering combustion: hydrogen engines. *Proc IEEE.* 2012;100:427-439. <https://doi.org/10.1109/JPROC.2011.2150190>

[123] Voelcker J. Hydrogen fuel-cell vehicles: everything you need to know. *Car Driv.* 2024. <https://www.caranddriver.com/features/a41103863/hydrogen-cars-fcev/>

[124] Vogel C. Wasserstoff-Dieselmotor mit Direkteinspritzung, hoher Leistungsdichte und geringer Abgasemission: Teil 1: Konzept. *MTZ – Mot Z.* 1999;60:704-708. <https://doi.org/10.1007/BF03226534>

[125] Wallner T, Lohsebusch H, Gurski S, Duoba M, Thiel W, Martin D et al. Fuel economy and emissions evaluation of BMW Hydrogen 7 Mono-Fuel demonstration vehicles. *Int J Hydrot Energy.* 2008;33:7607-7618. <https://doi.org/10.1016/j.ijhydene.2008.08.067>

[126] Wang H, You X, Ameya JV, Davis SG, Laskin A, Egolfopoulos F et al. USC Mech Version II. High-temperature combustion reaction model of  $H_2/CO/C_1-C_4$  compounds. 2007.

[127] Waseem M, Amir M, Lakshmi GS, Harivardhagini S, Ahmad M. Fuel cell-based hybrid electric vehicles: An integrated review of current status, key challenges, recommended policies, and future prospects. *Green Energy Intell Transp.* 2023;2:100121.  
<https://doi.org/10.1016/j.geits.2023.100121>

[128] Waseem M, Lakshmi GS, Sreeshobha E, Khan S. An electric vehicle battery and management techniques: comprehensive review of important obstacles, new advancements, and recommendations. *Energy Storage Sav.* 2025;4:83-108.  
<https://doi.org/10.1016/j.enss.2024.09.002>

[129] Welsch R. Rigorous close-coupling quantum dynamics calculation of thermal rate constants for the water formation reaction of H<sub>2</sub> + OH on a high-level PES. *J Chem Phys.* 2018;148:204304. <https://doi.org/10.1063/1.5033358>

[130] Wesołowski M, Hamid M, Mońska P, Janicka A. Analysis of the potential of electro-waste as a source of hydrogen to power low-emission vehicle powertrains. *Combustion Engines.* 2024;196:126-133.  
<https://doi.org/10.19206/CE-169494>

[131] Wooldridge MS, Hanson RK, Bowman CT. A shock tube study of the OH + OH → H<sub>2</sub> O + O reaction. *Int J Chem Kinet.* 1994;26:389-401.  
<https://doi.org/10.1002/kin.550260402>

[132] Wróbel K, Wróbel J, Tokarz W, Lach J, Podśadni K, Czerwiński A. Hydrogen internal combustion engine vehicles: a review. *Energies.* 2022;15:8937.  
<https://doi.org/10.3390/en15238937>

[133] Xiao T, He A, Pei X, Pan M, Wang X, Hu Z. Research on hydrogen-fueled turbojet engine control method based on model-based design. *Processes.* 2023;11:3268.  
<https://doi.org/10.3390/pr11123268>

[134] Zadrag R, Socik P, Kniaziewicz T, Zacharewicz M, Bogdanowicz A, Wirkowski P. Analysis of simulated dynamic loads of a ship propulsion system of a non-conventional power system. *Combustion Engines.* 2024;197(2):158-168.  
<https://doi.org/10.19206/CE-184139>

[135] Zhao F, Sun B, Yuan S, Bao L, Wei H, Luo Q. Experimental and modeling investigations to improve the performance of the near-zero NO<sub>x</sub> emissions direct-injection hydrogen engine by injection optimization. *Int J Hydrom Energy.* 2024;49:713-724. <https://doi.org/10.1016/j.ijhydene.2023.09.039>

[136] Zhou A. Review of hydrogen fuel cell vehicle research. *Acad J Eng Technol Sci.* 2022;5.  
<https://doi.org/10.25236/AJETS.2022.050908>

[137] Zhu D, Shu B. Recent progress on combustion characteristics of ammonia-based fuel blends and their potential in internal combustion engines. *Int J Automot Manuf Mater.* 2023;20. <https://doi.org/10.53941/ijamm0201001>

[138] Zsély IGy, Zádor J, Turányi T. Uncertainty analysis of updated hydrogen and carbon monoxide oxidation mechanisms. *Proc Combust Inst.* 2005;30:1273-1281.  
<https://doi.org/10.1016/j.proci.2004.08.172>

Mariusz J. Nieścioruk, MEng. – mniescioruk AEI, Poland.  
e-mail: [mariusz.j@niescioruk.eu](mailto:mariusz.j@niescioruk.eu)

Prof. Andrei-Alexandru Boroiu, DSc., DEng. – Faculty of Mechanics and Technology, National University of Science and Technology, Politehnica Bucharest, Romania.  
e-mail: [andrei.boroiu@upb.ro](mailto:andrei.boroiu@upb.ro)

Prof. Gustavo Ozuna – Department of Industrial Engineering and Systems, Hermosillo 83000, University of Sonora, Mexico.  
e-mail: [gozuna@industrial.uson.mx](mailto:gozuna@industrial.uson.mx)



Prof. Agustín Brau Ávila, DSc., DEng. – Department of Industrial Engineering and Systems, Hermosillo 83000, University of Sonora, Mexico.

e-mail: [agustin.brau@unison.mx](mailto:agustin.brau@unison.mx)



Przemysław Kubiak, DSc., DEng. – Institute of Vehicles and Construction Machinery Engineering, Warsaw University of Technology, Poland.  
e-mail: [przemyslaw.kubiak@pw.edu.pl](mailto:przemyslaw.kubiak@pw.edu.pl)



Marek Wozniak, DEng. – Department of Vehicles and Fundamentals of Machine Design, Lodz University of Technology, Poland.  
e-mail: [marek.wozniak.1@p.lodz.pl](mailto:marek.wozniak.1@p.lodz.pl)



Krzysztof Siczek, DSc., DEng. – Department of Vehicles and Fundamentals of Machine Design, Lodz University of Technology, Poland.  
e-mail: [ks670907@p.lodz.pl](mailto:ks670907@p.lodz.pl)

